Magnetic order in the random-field Ising film $Fe_{0.52}Zn_{0.48}F_2$

D. P. Belanger, J. Wang, Z. Slanič, and S-J. Han
Department of Physics, University of California, Santa Cruz, California 95064

R. M. Nicklow
Solid State Division, Oak Ridge National Laboratory, Oak Ridge, Tennessee 37831

M. Lui
Hughes Research Laboratories, 3011 Malibu Canyon Road, Malibu, California 90265

C. A. Ramos
Centro Atómico Bariloche, 8400 Bariloche, Rio Negro, Argentina

D. Lederman
Department of Physics, University of California, San Diego, La Jolla, California 92093-0319
(Received 20 June 1995)

The extinction-free neutron scattering for a 3.4 μm epitaxial film of the dilute antiferromagnet $Fe_{0.52}Zn_{0.48}F_2$ has been studied near the (100) antiferromagnetic Bragg point. For the $H=0$ Bragg scattering we observe the random-exchange Ising model behavior $I\sim|t|^{2\beta}$ with $\beta=0.35$. For $0<H\leqslant 4.5$ T the random-field Ising peak intensity vs T has the opposite curvature from the $H=0$ case near $T_c(H)$. We argue that this has to do with the formation of two weakly interacting, interpenetrating, antiferromagnetically ordered domains with interfaces primarily falling on vacancy sites. [S0163-1829(96)02329-6]

Dilute Ising antiferromagnets have proven ideal for the study of the random-field Ising model (RFIM). Extensive experimental studies have been made of the $d=3$ RFIM transition over the past decade.[1,2] Scattering results near the transition temperature in a magnetic field, $T_c(H)$, have proven difficult to interpret, however, since extinction effects cause the Bragg scattering intensity to saturate in bulk crystals. To eliminate extinction effects, we fabricated a 3.4 μm film of $Fe_{0.52}Zn_{0.48}F_2$ epitaxially grown onto a ZnF_2 substrate. This has allowed a comprehensive characterization of the small-q scattering behavior in dilute antiferromagnets in applied fields.

The Imry-Ma domain-wall scaling arguments[3] applied to a ferromagnet with a random field yield the correct conclusion that the $d=3$ RFIM has a phase transition to long-range order, as was subsequently proven rigorously.[4,5] It has been argued that the dilute antiferromagnet in a uniform field is equivalent to the uniform ferromagnet with an applied random field,[6] at least regarding its equilibrium static critical behavior. The Imry-Ma-type pictures may break down at large dilution in antiferromagnets. The presence of a large number of vacancies greatly reduces the domain-wall energy cost, since domain walls form predominantly at the vacancy sites. Hence, the analogy between the ferromagnetic and antiferromagnetic RFIM may not be valid for large antiferromagnetic dilution. Mean-field simulations[7] of dilute antiferromagnets indicate that the free energy is lower for antiferromagnetic long-range order at low T, but near $T_c(H)$ the free energy is lower for a domainlike state. Cooling a dilute antiferromagnet in a field [field cooling (FC)] leads to fractal-like domain structure at low temperatures, as shown by Nowak and Usadel[8] in computer simulations. The antiferromagnetic lattice essentially breaks into two nearly static long-range antiferromagnetic ''domains'' of equal volume which, because of the large number of vacancies, are extremely interpenetrating but have little interaction with each other.[8,9] Percolating fractal-like fluctuating domains have also been observed[10] very close to the transition temperature in the ferromagnet with random fields as well as in pure magnets. However, in the case of the dilute antiferromagnet we find the net magnetization of the sample becomes zero very rapidly as $T_c(H)$ is approached after first cooling in zero field to establish long-range order [zero-field cooling (ZFC)] and the domain structure is almost completely irreversible. We will argue that the domain structure is in fact characteristic of the behavior near $T_c(H)$ regardless of whether the sample is FC or ZFC. The ZFC behavior, which shows long-range order at low T, evolves so rapidly toward this nearly static domain structure as T increases toward $T_c(H)$ that the Bragg scattering decrease is dominated by the formation of the two interpenetrating domains rather than the loss of long-range order due to critical fluctuations as would be the case for transitions in pure magnets.

The $Fe_{0.52}Zn_{0.48}F_2$ film was grown on a (001) ZnF_2 substrate along the (001) direction by molecular-beam epitaxy. The details of the growth process have been described previously.[11] X-ray rocking curve line widths, approximately 0.1° for Cu target radiation, show the film to be of extremely high quality, limited only by the substrate quality and a small distribution in the relative Fe/Zn concentration of less than 0.5%. The concentration was estimated from the x-ray Bragg scattering angle to be $x=0.46$ by linearly interpolating between the FeF_2 and ZnF_2 Bragg angles. The concentration was determined to be $x=0.52$ from the $H=0$ transition tem-

perature T_N, which is known to vary linearly with x for $x>0.4$. The excellent film growth quality is due in part to the nearly identical a-axis lattice parameters of $Fe_{0.52}Zn_{0.48}F_2$ and ZnF_2 ($\delta a/a<0.002$) and partly due to careful substrate surface preparation. The etch polishing also avoids spurious scattering effects that have been observed[12,13] in $Mn_{0.75}Zn_{0.25}F_2$ when the surface defects are numerous. The 3.4 μm film thickness constitutes more than 10 000 lattice spacings. Hence, we expect $d=3$ critical behavior. The behavior of a pure FeF_2 epitaxial film of thickness 0.8 μm has been shown in a previous study to approximately follow the $d=3$ Ising model[14] with no extinction effects. As discussed below, high-resolution measurements establish the $d=3$ Ising critical behavior with no appreciable rounding for $|t|>10^{-2}$, where $t=(T-T_N)/T_N$. Hence, the dilute film should accurately exhibit the correct critical behavior of the $d=3$ RFIM in a dilute antiferromagnet.

The neutron-scattering experiments were performed at the Oak Ridge National Laboratory using the HB2 spectrometer in a two-axis configuration at the High Flux Isotope Reactor. We used the (111) reflection of silicon to monochromate the beam at 14.8 meV. Two collimation configurations were used to collect data. For the first, which we will refer to as the low-resolution configuration, the collimation was 50 min of arc before the monochromator, 40 between the monochromator and sample, and 40 after the sample. The transverse half width at half maximum (HWHM) resolution in this case is 0.0034 r.l.u. A higher resolution configuration differed in that the collimation before and after the sample was 20 minutes of arc. The resulting HWHM transverse resolution is 0.0020 r.l.u. A pyrolitic graphite filter reduced higher energy neutron contamination. All of the fits used in the analysis of the scattering intensities vs q were done by folding in the measured resolution scans.[15] The results shown in the figures were obtained using transverse scans over a very narrow range of q about the Bragg scattering point. Longitudinal scans were also made but do not alter our conclusions and so are not discussed.

In a preliminary report[16] we discussed the low-resolution behavior of the Bragg intensity and the ZFC behavior at $H=2.0$ T. The zero-field data for the Bragg intensity vs T showed apparent rounding of the expected critical behavior of the staggered magnetization. At that time, the source of the rounding was not clear. This limited the impact of the preliminary report since it was unclear to what extent the rounding could be indicative of poor sample quality. In this report, with higher resolution data, we are able to show that the rounding was almost entirely an effect of the resolution; we see no significant rounding in the higher resolution data for $|t|>10^{-2}$. Hence, the order-parameter critical behavior is comparable in quality to that observed in many high-quality bulk crystals. Hence, there is every indication that sample quality is not a factor influencing the conclusions we draw from the experimental results. In this study, we also compare the line shapes for $H>0$ upon FC and FH (heating after FC) and compare the profiles to those reported earlier for ZFC. Finally, in this report we demonstrate the irreversibility of the ZFC line shape and show that significant hysteresis occurs only for very small q.

We first discuss the higher resolution results in zero applied field and establish that we can observe extinction-free

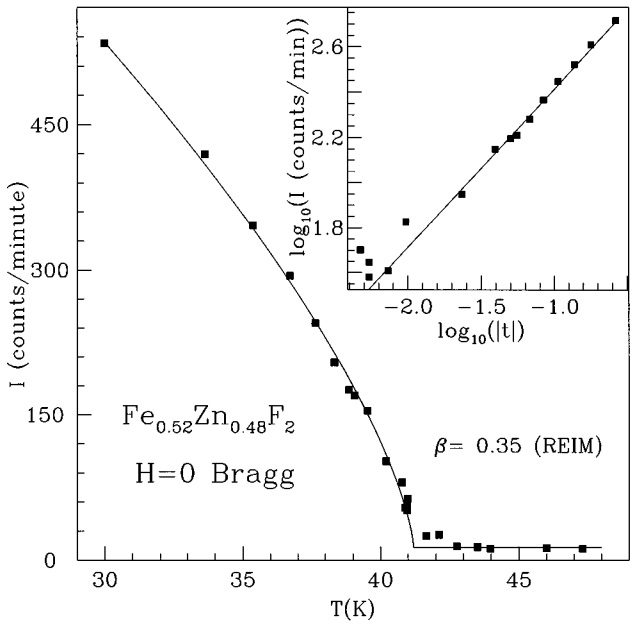

FIG. 1. The Bragg scattering amplitude vs T at the antiferromagnetic Bragg point for $H=0$ in the high-resolution configuration. The REIM order-parameter power law is represented by the solid curve. The inset shows the logarithm of the Bragg scattering amplitude, less the background, vs the logarithm of $|t|$. The solid curve represents $\beta=0.350$. The lack of rounding for $|t|>10^{-2}$ demonstrates the very high quality of the epitaxial film.

$d=3$ random-exchange Ising model (REIM) behavior in the Bragg intensity with no appreciable rounding. Figure 1(a) from the preliminary report[16] shows the transverse (100) Bragg scattering line shapes at $H=0$ for various temperatures using the lower resolution configuration. The widths of the peaks are instrumental resolution limited. Scattering from thermal fluctuations, represented by the usual Lorentzian line shape,[18] is too weak to be separated from background intensity. Hence, the data were fit to a Gaussian line shape, which represents long-range antiferromagnetic order, plus a q-independent background term. Figure 1(b) of the preliminary report shows the Bragg scattering amplitude vs T obtained from transverse scans. The Bragg intensities show rounding near $T_c(H)$. In the present study, in order to determine the source of the rounding, we reexamined the line shapes with the higher resolution configuration described above. The line shapes are again Gaussian, with little evidence for a Lorentzian component. The fitted intensities vs T from the high-resolution scans are shown in Fig. 1 of this report with the curve being the sum of a random-exchange Ising model (REIM) power law,

$$I_B \sim m_s^2 = m_0 |t|^{2\beta} \tag{1}$$

with $\beta=0.35$ (Ref. 17) and a small T-independent background term. The rounding is much smaller for higher resolution since higher resolution enhances the Bragg scattering intensity relative to that from thermal fluctuations, represented by a Lorentzian component. The rounding occurs at reduced temperatures on the order of $|t|<10^{-2}$. The small remaining rounding may well be from the small thermal fluctuation contributions still persisting with higher resolution.

The lack of rounding is shown most clearly in the Fig. 1 inset where the logarithm of the Bragg intensity data is plotted versus the logarithm of $|t|$. The small, constant background has been subtracted from both the data and fit in the inset. The lack of rounding from concentration gradients, and the ability to show the correct critical behavior [Eq. (1)] demonstrates clearly that the epitaxial film is of very high quality both crystallographically and in the smallness of any concentration gradient. The present $H=0$ experiments show that the film is clearly suitable for detailed Bragg intensity critical behavior studies with $H>0$. The rounding of the scattering intensities vs T observed for $H>0$, discussed below, must therefore be intrinsic to the $d=3$ Ising random-field behavior of dilute antiferromagnets films and is not an artifact of poor sample quality.

We studied the RFIM behavior for $H=1.5, 2.0, 3.0$ and 4.5 T. Results for ZFC at $H=2.0$ T in the lower resolution configuration were discussed previously.[16] Here we add a discussion of FC and FH results for $H=2.0$ T at that resolution and results for $H=4.5$ T obtained at this and the higher resolution configurations. Only the behavior at $H=2.0$ and 4.5 T will be discussed in detail. The data at $H=1.5$ and 3.0 T show similar behaviors and need not be discussed.

The hysteresis exhibited by dilute antiferromagnets in applied fields is well known.[18] FC never achieves long-range order since the system never fully equilibrates while passing through a spin-glass-like phase[19] between $T_{\rm eq}(H)$, above which no hysteresis is observed, and $T_c(H)$. The ZFC procedure results in longer-range order than the FC one and the critical behavior is sharper after ZFC compared with FC. We observe the hysteresis in the scattering intensity vs q in transverse scans. $H=2.0$ T scans obtained upon ZFC in the low-resolution configuration are shown at various temperatures in Fig. 2(a). For comparison, similar scans obtained upon FC are shown in Fig. 2(b). For both ZFC and FC there are large, clearly non-Gaussian tails not present for $H=0$. Mean-field theory suggests[18] that for the RFIM, neglecting the weak Lorentzian thermal fluctuation contribution,

$$S(q)\approx \frac{A}{(q^2+\kappa^2)^2}+M_s^2\delta(q) \qquad (2)$$

where κ is the inverse correlation length. The observed scattering intensity line shape would then be proportional to this function with experimentally determined resolution corrections.[15] With instrumental resolution corrections, the δ function Bragg scattering component, which represents long-range antiferromagnetic order, becomes a Gaussian peak with a width determined by the transverse resolution. A squared-Lorentzian component represents in the mean-field theory a nonuniformity in the staggered magnetization.[20–22] The non-Gaussian part of the line shape is more troublesome to analyze since the resolution corrections involve all components of the resolution ellipsoid. The vertical and transverse resolutions are much larger and more significant than the transverse one. Because the large resolution corrections depend on the line shape itself, it proves very difficult to determine the proper line shape for the non-Bragg scattering directly from the scattering data. In the absence of a proper line shape from theory, we are forced to use the mean-field representation of $S(q)$ in Eq. (2). However, we find significant problems with this form, as we shall note, and it should only be considered to be a way of parameterizing the behavior. This is the same situation found for scattering in a bulk crystal at a similar concentration.[23]

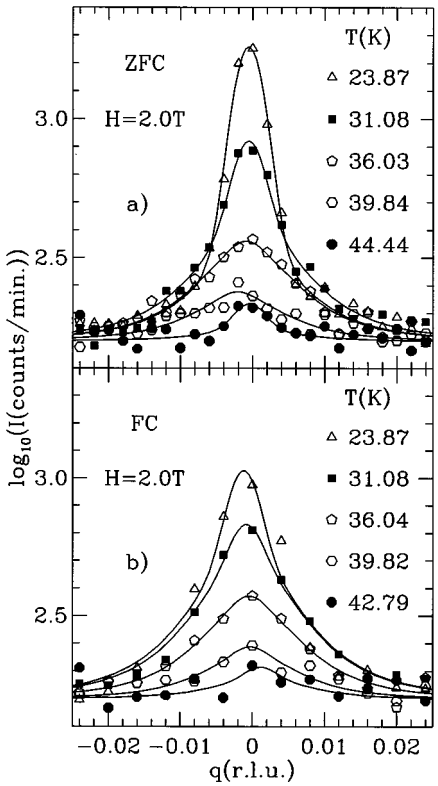

FIG. 2. The scattering behavior near the antiferromagnetic Bragg point (100) for $H=2.0$ T in the low-resolution configuration: (a) The logarithm of the ZFC scattering intensity vs q for several temperatures. The solid curves represent fits to the sum of a squared Lorentzian, a resolution limited Gaussian and a background term; (b) The logarithm of the FC scattering intensity vs q for several temperatures. The solid curves are fits as described above.

We analyzed the data using Eq. (2), where κ is arbitrarily fixed to the value obtained at the lowest temperature at which measurements were made. This was necessary since the widths obtained in fits are close to the transverse resolution. Fixing the width made the results for the fitted parameters more consistent, but did not change their qualitative behaviors. The near-resolution widths point to the difficulty in determining the correct line shape from the data scans and to the inadequacy of Eq. (2), where κ should vary with T. What we can determine directly is that the line shapes are extremely narrow; all of the scans show significant scattering only for $q<0.03$ r.l.u. and all the peaks appear nearly resolution limited. The fits to the scattering data also include a constant background term that is fixed to the value determined at the lowest temperature.

The ZFC and FC Bragg amplitudes for $H=2.0$ T are shown vs T in Fig. 3(a). $T_c(H)$ in this and subsequent figures is taken to be appropriately shifted downward from the zero-field T_N using the temperature shift determined[24] from bulk crystal measurements[1] on $Fe_xZn_{1-x}F_2$. It is evident that near $T_c(H)$ structure at the longest length scales (small q) exhibits strong hysteresis; the FC Bragg intensity is clearly much smaller at low temperatures compared to the ZFC. The

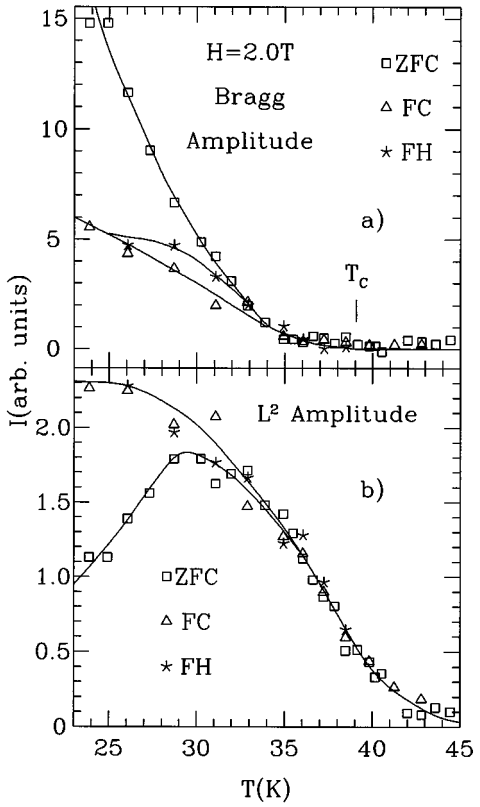

FIG. 3. The fitted amplitudes for $H=2.0$ T for the low-resolution configuration: a) The Bragg amplitude vs T; b) The squared-Lorentzian amplitude vs T.

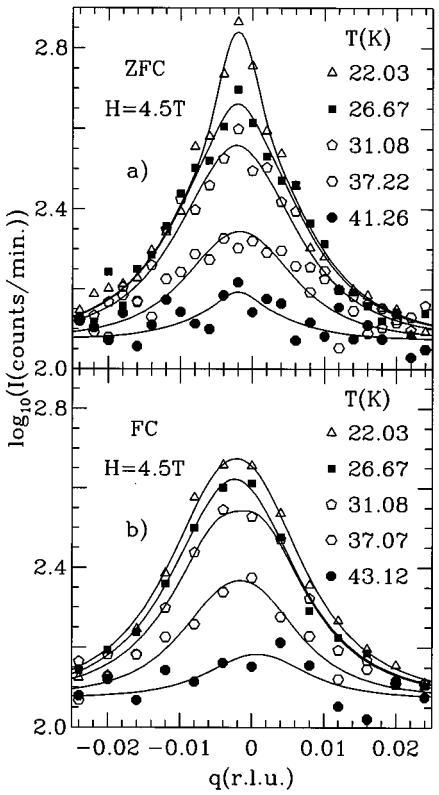

FIG. 4. The scattering behavior near the antiferromagnetic Bragg point (100) for $H=4.5$ T in the low-resolution configuration: (a) The logarithm of the ZFC scattering intensity vs q for several temperatures. The solid curves are fits as described for Fig. 2(b). The logarithm of the FC scattering intensity vs q for several temperatures. The solid curves are fits as described above.

most striking aspect of the Bragg intensity temperature dependence is seen in the ZFC fitting results. The curvature of the intensity versus T is *opposite* to that observed in zero field. If interpreted in terms of Eq. (1), β would have to be much larger than 1/2, the mean-field value, a rather peculiar result. It should be emphasized that the reversed curvature observed in the Bragg scattering amplitude is clearly apparent in the raw (100) intensity data. No matter how it is analyzed, the dramatic decrease in the intensity at $q=0$ is quite unusual. As we discuss below, it is not clear that the observed Bragg intensity is a good measure of the order-parameter critical behavior. In addition to the ZFC and FC procedure, we show in Fig. 3 the behavior for a third procedure, FH, which is simply heating after FC. The FH behavior for the Bragg intensity is intermediate between the FC and ZFC behaviors and most likely represents the movement from the metastable FC domains, which lack order on the longest length scales, towards the ZFC structure upon heating. None of these procedures yield a perceptible difference close to $T_c(H)$ since all the Bragg intensities are close to zero.

Figure 3(b) shows the $H=2.0$ T ZFC, FC, and FH squared-Lorentzian amplitudes, obtained from the fits of the data to Eq. (2). The ZFC amplitude has a maximum near $T=30$ K and decreases smoothly through $T_c(H)$ as T is increased. The $H=2.0$ T FC squared-Lorentzian amplitude increases monotonically as T is lowered. The FH behavior closely follows the FC behavior, indicating that FH only differs from the FC behavior at the largest length scales. Near $T_c(H)$ the ZFC, FC, and FH amplitudes are indistinguishable, suggesting that the structure causing the tails is not history dependent near $T_c(H)$ for length scales shorter than the resolution limit.

Very similar behavior is observed for $H=4.5$ T. Fig. 4(a) and 4(b) show the ZFC and FC line shapes, respectively, for the low-resolution configuration for comparison to the $H=2.0$ T data. The scales are directly comparable to those of the $H=2.0$ T figures since the experimental configurations and counting times are the same. Relative to the $H=2.0$ T case, it appears that less of the line shape in the ZFC case comes from the longest length scales. Again, upon FC the scattering intensity at the longest length scales seen in the ZFC scan is not recovered. In Figs. 5(a) and 5(b) we show the Bragg and squared-Lorentzian amplitudes obtained at $H=4.5$ T using the high-resolution configuration. As can be seen, the squared-Lorentzian amplitude obtained from Eq. (2) is nearly identical for $T>28$ K, i.e., throughout the critical range. The Bragg component, on the other hand, shows extreme hysteresis; the FC Bragg intensity hardly grows at all as T decreases.

The shapes of the Bragg intensity versus T curves belie the sharpness of the transitions for $H>0$. The behavior is consistent with that observed[23] in bulk samples, where the ZFC Bragg intensities are unusually small near $T_c(H)$. They are so small, in fact, that the sharp peaks in the fluctuation scattering at $T_c(H)$ are quite clearly observed in the bulk

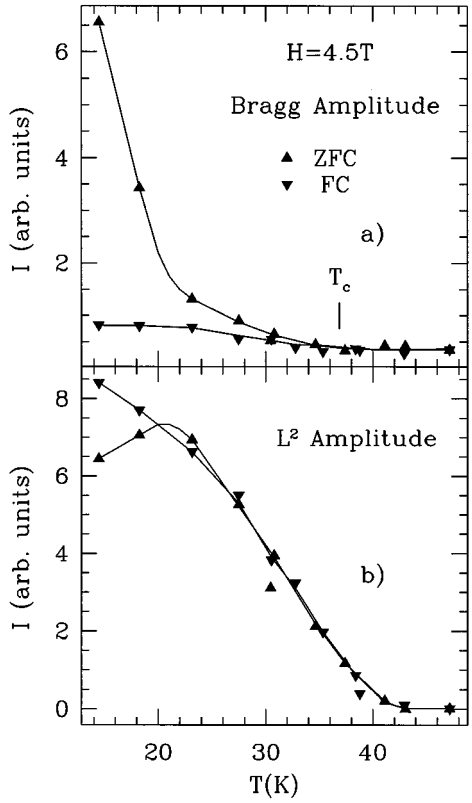

FIG. 5. The fitted amplitudes for $H=4.5$ T for the high-resolution configuration: (a) The Bragg amplitude vs T; (b) the squared Lorentzian amplitude vs T.

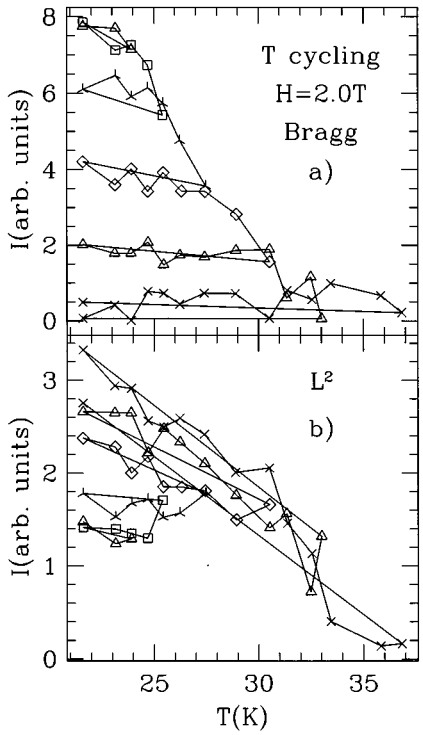

FIG. 6. The scattering Bragg and squared-Lorentzian amplitudes vs T after ZFC to $T=21.6$ K and raising the field to $H=2.0$ T are shown in (a) and (b), respectively. The temperature was incrementally increased to the temperatures shown and the intensities obtained from a fit to the scan are plotted versus T. After reaching a maximum temperature, the sample temperature was lowered to $T=21.6$ K. The temperature was then increased incrementally to a new higher temperature, with the intensities shown for each temperature, and again the sample temperature was lowered to $T=21.6$ K. The process was repeated until the Bragg scattering amplitude was negligible, still well below $T_c(H)\approx 39$ K. Each temperature cycle is represented by a different symbol. The Bragg amplitude never increases significantly upon cooling. The envelope of the Bragg amplitudes at the highest T for each cycle follows the ZFC behavior in Fig. 3 quite well. The corresponding squared-Lorentzian amplitudes increase for each temperature cycling. The squared-Lorentzian amplitudes do increase whenever the temperature is decreased, indicating that they probably represent some of the magnetic ordering.

crystals.[23] Normally, the Bragg scattering completely obscures the fluctuation peaks. It is clear as well from other bulk crystal measurements that very sharp critical behavior occurs, for example in the specific heat and susceptibility.[1] Since we have shown the $H=0$ transition in the film to be extremely sharp, the $H>0$ transitions should be comparably sharp.

The irreversibility in the ZFC Bragg and squared-Lorentzian intensities is demonstrated in Figs. 6(a) and 6(b), respectively. The Bragg intensity versus T is shown for $H=2.0$ T, beginning at $T=21.6$ K after establishing long-range antiferromagnetic order via ZFC. The temperature is incrementally increased to each point for which the Bragg and squared-Lorentzian intensities are shown until a maximum temperature after which the sample is cooled to the $T=21.6$ K. The process is repeated several times, each time increasing the temperature to a higher temperature before decreasing it. All of the data shown in Fig. 6 are below $T_c(H)\approx 39$ K. Data were also taken in a procedure in which the sample was incrementally cooled in several steps rather than cooling in one temperature change, but the data look essentially identical. The squared-Lorentzian intensity is shown in Fig. 6(b) for precisely the same scans as in Fig. 6(a). Several important points can be seen from the hysteretic behavior. The envelope of the Bragg intensities at the temperatures achieved just before cooling follows quite well the behavior of the sample when it is simply heated after ZFC. Upon cooling, very little of the low-temperature $q=0$ intensity is recovered. Furthermore, the intensity does not significantly decrease again until the previous highest temperature is surpassed. Interestingly, the relative Bragg intensity after cooling from the highest temperature, which is still below $T_c(H)$, is lower than the FC intensity. These observations indicate that whatever configuration is achieved by heating cannot evolve towards the original long-range order induced by ZFC. No significant time dependence is observed for any of these intensities. This is not surprising considering that the domain structure does not evolve appreciably even when the field is decreased to zero.[8,9] The ZFC squared-Lorentzian amplitudes increase whenever T is lowered and are higher for all T each time a new maximum temperature is reached. Hence, as T is decreased, the system cannot achieve significantly more order at $q=0$ but can increase the order contributing to scattering at $q>0$.

We suggest that all of the observed behavior is consistent with the system forming interpenetrating, weakly interacting domains which form as $T_c(H)$ is approached from below.

There are so many vacancies that this process costs little in terms of domain-wall energy. The domain formation would decrease the Bragg scattering very quickly at temperatures well below the transition to paramagnetism within the domains. The unusual line shapes, which do not seem to correspond to the predicted mean-field behavior, could also be explained by the interpenetrating domain structure. Since we know that domain structure is quite irreversible, this would also explain the strong irreversibility after ZFC.

The irreversible behavior observed after ZFC is quite in accord with the hysteresis observed between FC and ZFC at $T_{\rm eq}(H)$. It is well-known that the FC configurations do not lead to sharp critical behavior and have finite Bragg scattering widths at low temperatures, while ZFC yields much sharper critical behavior and resolution limited Bragg peaks below $T_c(H)$. Since we have now shown that long-range antiferromagnetic order is not recovered upon cooling at any temperature, it is clear that the FC procedure suffers only in that the hysteresis sets in above $T_c(H)$ where short-range antiferromagnetic fluctuations are frozen in and, hence, long-range order does not develop below $T_c(H)$. The ZFC procedure, though resulting in the interpenetrating structure as $T_c(H)$ is approached, always has structures on a much longer length scale than in the FC procedure. It is not clear from the present study whether the long-range antiferromagnetic order is the equilibrium state everywhere below $T_c(H)$, or whether the interpenetrating domain state achieves a true equilibrium state with lower free energy near $T_c(H)$. The lack of observable time dependence in the Bragg scattering leaves this question open. The critical-like antiferromagnetic fluctuations observed[23] in bulk samples very close to $T_c(H)$ must be occurring on the interpenetrating domain structure and occur when the Bragg intensity is essentially zero. The same is true of all other critical behavior observations, including the specific heat.[1]

The decrease in the antiferromagnetic order with increasing T cannot be a simple matter of nonequilibrium behavior or slow relaxation, as has been argued previously[12] for $Mn_xZn_{1-x}F_2$, a system which otherwise exhibits random-field behavior similar to $Fe_xZn_{1-x}F_2$. If this were so, one would expect the ZFC long-range order to persist to higher temperatures than $T_c(H)$. In our case, however, the long-range antiferromagnetic order is essentially zero by the time $T_c(H)$ is reached after ZFC. It was stated that for $Mn_xZn_{1-x}F_2$ the peak in critical behavior studies appears at the point of the most precipitous drop in the Bragg intensities versus T. Such an interpretation would be in stark contrast to the present experimental results in $Fe_xZn_{1-x}F_2$ which show that $T_c(H)$, as determined for example,[1] from specific heat, susceptibility measurements, or neutron-scattering critical fluctuation intensities, occurs far above the point where the intensity is dropping most rapidly. We believe the apparent disparity in the conclusions drawn from the $Mn_xZn_{1-x}F_2$ and $Fe_xZn_{1-x}F_2$ studies to be a consequence of a misidentification of $T_c(H)$ in the former study. When this is realized, the physical behavior of the two systems are completely consistent. The $Mn_xZn_{1-x}F_2$ sample used was taken from the same boule as the one used by Shapira, Oliveira, and Foner,[25] who used it in a careful, comprehensive study of the phase diagram. The zero-field transition of the two samples appears to be nearly identical, and the shifts in $T_c(H)$ with the applied field should therefore be the same. Field-insensitive carbon-glass thermometry removes any large uncertainties from field-dependent thermometry.[12] If one believes the accuracy of the phase diagram measured by Shapira *et al.* and transfers the field-induced shift in $T_c(H)$ to the Bragg scattering curves, it is clear that the susceptibility peaks, and consequently all other critical behavior peaks, occur at the point where the Bragg scattering approaches zero, not at the point of steepest slope, as suggested.[12] This is also confirmed by an experimental study[26] of the concentration dependence of the shift of $T_c(H)$ from T_N in $Mn_xZn_{1-x}F_2$. Interpolating to the concentration $x=0.75$, we can find the expected $T_c(H)$ appropriate to the x-ray study.[12] Using either of these two techniques, one finds, for example, that $T_c(6.0\ \mathrm{T})=43.0\pm0.1$ K, in disagreement with the assignment of $T_c(6.0\ \mathrm{T})$ to be where the most precipitous Bragg intensity drop takes place at $T\approx42.4$ K. With $T_c(6.0\ \mathrm{T})=43.0$ K, it is clear that the transition occurs when the Bragg intensity is zero, just as in the present study. Unfortunately, this does not fit the previously proposed physical picture developed to explain the scattering behavior in the $Mn_xZn_{1-x}F_2$ x-ray scattering studies,[12,13] which should be revised appropriately.

Piezomagnetic stress fields are another source of magnetic-field-induced domains in $Fe_xZn_{1-x}F_2$ systems.[27–30] A related effect, magnetostriction linear in H (inverse piezomagnetic effect), was used to measure β in the random-field system $Fe_xZn_{1-x}F_2$. This ''anomalous'' magnetostriction (which otherwise would be quadratic in the applied field) is driven by a magnetoelastic (ME) energy term of the form $E\propto\lambda\langle\sigma_{xy}(r)\rangle H_z M_{\rm stag} V$ where λ is a coupling constant, $\sigma_{xy}(r)$ is a stress field, H_z is the applied field, $M_{\rm stag}$ is the staggered magnetization, and V is a volume over which $\sigma_{xy}(r)$ is averaged.[31] If σ_{xy} is not caused by an external uniform stress, but by internal stresses, then antiferromagnetic (AF) domains may form to accommodate the stress field spatial variation. These AF domains will be created if the associated wall energy is smaller than the ME volume contribution. If large stresses are present, such as near rough surfaces,[13] the ME term may stabilize antiferromagnetic domains of a size determined by the competition between the ME term, the wall energy and the random-field interaction. These ME domains interfere with the development of random-field-induced domains. Not surprisingly this artifact disappears if the same sample is more carefully polished.[12] Epitaxial films of FeF_2 grown by similar methods as our sample, show that the effect of stresses in the rounding of the transition is diminished when compared with typical polishing procedures.[11] However, we cannot discard the formation of AF domains driven by the ME interaction in our sample. This is so, not only because we do not know the actual state of stress of the sample, but also because in FeF_2 ME terms are expected to be larger than in MnF_2. This could lead to small domain sizes, probably down to approximately 1000 Å. The resolution of the neutron-scattering scans is about 370 Å (Ref. 32) and we see a resolution-limited line shape at all fields after ZFC. Unless there is a wide range of domain structures, as there would be for the interpenetrating domains described by Nowak and Usadel, it is hard to account for the resolution-limited line shapes invoking only the piezomagnetic stress domains unless they are typically much larger

than 370 Å. The extremely small Bragg intensity near $T_c(H)$ for the epitaxial film is similar to the behavior observed in bulk crystals. Hence, we believe at this point that the domains responsible for the unusual Bragg intensity versus T behavior are primarily the intrinsic random-field-induced domains as seen in simulations and not piezomagnetic domains. We cannot rule out completely the influence of piezomagnetic domains, however. Further study of epitaxial films may help to elucidate this point.

Monte Carlo simulations of a uniform Ising ferromagnet with a random field[33,34] do not seem to show the unusual behavior seen in these experiments. This may be a result of the absence of vacancies which are numerous in dilute antiferromagnets. It should be possible to study the dilute antiferromagnet scattering behavior near the phase transition using Monte Carlo simulations. Such studies may further elucidate the unusual behavior we have observed and give some indication of a more appropriate scattering line shape to use in neutron-scattering data analysis.

In conclusion, we have argued that the interpenetrating domain structure observed in simulations of FC dilute antiferromagnets at low temperature is also relevant to the ZFC scattering profiles near $T_c(H)$. The structure probably occurs since the large number of vacancies allows the formation of the domains with little cost in domain-wall energy. The drastic drop in the Bragg scattering as $T_c(H)$ is approached from below is due to the formation of this structure after starting with the ZFC long-range order. All critical behavior takes place on this domain structure. It is important for future progress in understanding the critical behavior of the RFIM in dilute antiferromagnets to take this domain structure into account, perhaps even to the extent of rethinking what the precise order parameter is for dilute antiferromagnets in a field. It is not clear that the fractal nature of the domains, as demonstrated in simulations at low temperatures,[8] is necessarily a feature of the interpenetrating domains near $T_c(H)$. Further simulation studies and the analysis of much higher resolution neutron or x-ray scattering line shapes could characterize the structure distribution. There must be, however, a large range of structure sizes to account for both the large tails of the resolution-limited squared-Lorentzian-like scattering component and for the lack of a significant Bragg contribution. The interpenetrating domain structure, whether fractal-like or not, does explain the extraordinary decrease in the ZFC Bragg scattering. Below $T_c(H)$ it is clear that the line shapes are extremely narrow and should be related to the nature of the domain structure. Magnetic x-ray studies,[12] which have the advantage of much higher instrumental q resolution, indicate that the line shapes may be much sharper than can be possibly indicated by present neutron-scattering experiments. If the order parameter is still strictly taken to be antiferromagnetic order, it must be extremely small near $T_c(H)$, which is odd in light of the critical behavior in other experiments such as the specific heat which indicate changes in entropy comparable to the zero-field transitions. Finally, one should keep in mind that the transitions for $H>0$ are not observed in equilibrium because of the extreme critical slowing[35] down near T_c. The consequences the nonequilibrium nature of the RFIM transitions in dilute antiferromagnets needs to be further explored theoretically.

Fruitful discussions with W. Kleemann are gratefully acknowledged. This research was supported in part by Department of Energy Grant No. DE-FG03-87ER45324 and by the Division of Materials Sciences, U.S. Department of Energy, under Contract No. DE-AC05-84OR21400 with Martin Marietta Energy Systems, Inc.

[1] D. P. Belanger and A. P. Young, J. Magn. Magn. Mater. **100**, 272 (1991), and references therein.
[2] W. Kleemann, Int. J. Mod. Phys. B **7**, 2469 (1993).
[3] Y. Imry and S. K. Ma, Phys. Rev. Lett. **35**, 1399 (1975).
[4] J. Bricmont and A. Kupiainen, Phys. Rev. Lett. **59**, 1829 (1987).
[5] J. Z. Imbrie, Phys. Rev. Lett. **53**, 1747 (1984).
[6] J. L. Cardy, Phys. Rev. B **29**, 505 (1984).
[7] H. Yoshizawa and D. P. Belanger, Phys. Rev. B **30**, 5220 (1984).
[8] U. Nowak and K. D. Usadel, Phys. Rev. B **44**, 7426 (1991); **46**, 8329 (1992); Physica A **191**, 203 (1992).
[9] S-J. Han and D. P. Belanger, Phys. Rev. B **46**, 2926 (1992).
[10] J. L. Cambier and M. Nauenberg, Phys. Rev. B **34**, 7998 (1986); **34**, 8071 (1986).
[11] M. Lui, A. R. King, V. Jaccarino, and G. L. Snider, Phys. Rev. B **40**, 4898 (1989); M. Lui, Ph.D. thesis, UCSB, 1989.
[12] J. P. Hill, Q. Feng, R. J. Birgeneau, and T. R. Thurston, Phys. Rev. Lett. **70**, 3655 (1993); Z. Phys. B **92**, 285 (1993).
[13] J. P. Hill, T. R. Thurston, R. W. Erwin, M. J. Ramstad, and R. J. Birgeneau, Phys. Rev. Lett. **66**, 3281 (1991).
[14] D. P. Belanger, M. Lui, and R. W. Erwin, in *Magnetic Ultrathin Films: Multilayers and Surfaces/Interfaces and Characterization*, edited by B. T. Jonker, S. A. Chambers, R. F. C. Farrow, C. Chappert, R. Clarke, W. J. M. de Jonge, T. Egami, P. Grünberg, K. M. Krishnan, E. E. Marinero, C. Rau, and S. Tsunashima, MRS Symposia Proceedings No. 313 (Materials Research Society, Pittsburgh, 1993), p. 755.
[15] D. P. Belanger and H. Yoshizawa, Phys. Rev. B **35**, 4823 (1987).
[16] D. P. Belanger, J. Wang, Z. Slanič, S.-J. Han, R. M. Nicklow, M. Lui, C. A. Ramos, and D. Lederman, J. Magn. Magn. Mater. **140-144**, 1549 (1995).
[17] N. Rosov, A. Kleinhammes, P. Lidbjork, C. Hohenemser, and M. Eibschutz, Phys. Rev. B **37**, 3265 (1988).
[18] D. P. Belanger, Phase Transitions **11**, 53 (1988).
[19] M. Mezard and R. Monasson, Phys. Rev. B **50**, 7199 (1994).
[20] R. A. Pelcovits and A. Aharony, Phys. Rev. B **31**, 350 (1985).
[21] S. W. Lovesey, J. Phys. C **17**, 6113 (1984).
[22] P. M. Richards, Phys. Rev. B **30**, 2955 (1984).
[23] D. P. Belanger, A. R. King, V. Jaccarino, and R. M. Nicklow, Phys. Rev. Lett. **59**, 930 (1987).
[24] I. B. Ferreira, A. R. King, and V. Jaccarino, Phys. Rev. B **43**, 10 797 (1991).
[25] Y. Shapira, N. F. Oliveira, Jr., and S. Foner, Phys. Rev. B **30**, 6639 (1984).
[26] C. A. Ramos, A. R. King, and V. Jaccarino, Phys. Rev. B **37**, 5483 (1988).
[27] C. A. Ramos, A. R. King, V. Jaccarino, and S. M. Rezende, J. Phys. (Paris) Colloq. **49**, C8-1241 (1988).
[28] J. Kushauer, W. Kleemann, J. Mattsson, and P. Nordblad, Phys. Rev. B **49**, 6346 (1994).

[29] J. Kushauer, C. Binek, and W. Kleemann, J. Appl. Phys. **75**, 5856 (1994).
[30] J. Baruchel, A. Draper, M. El Kadiri, G. Fillion, M. Maeder, P. Molho, and J. L. Proteseil, J. Magn. Magn. Mater. **C8**, 1895 (1988).
[31] A. S. Prokhorov and E. G. Rudashevskii, JETP Lett. **10**, 110 (1969).
[32] The resolution is given in units of Å, not Å $/2\pi$, as is often used.
[33] H. Rieger and A. P. Young, J. Phys. A **26**, 5279 (1993).
[34] H. Rieger, Phys. Rev. B **52**, 6659 (1995).
[35] C. Binek, S. Kuttler, and W. Kleemann, Phys. Rev. Lett. **75**, 2412 (1995).